

RESEARCH ARTICLE

Long-Term Variability of Fog in Poland

Olga Zawadzka-Manko  | Krzysztof M. Markowicz 

Institute of Geophysics, Faculty of Physics, University of Warsaw, Warsaw, Poland

Correspondence: Olga Zawadzka-Manko (olga.zawadzka@fuw.edu.pl)**Received:** 13 February 2024 | **Revised:** 20 December 2024 | **Accepted:** 29 January 2025**Funding:** This work was supported by Polish Grant No. 2017/27/B/ST10/00549 of the National Science Centre coordinated by the Institute of Geophysics, Faculty of Physics, University of Warsaw.**Keywords:** aerosol | climate change | fog | relative humidity | smog | visibility

ABSTRACT

Fog phenomena are frequent natural hazards, sensitive to meteorological parameters, with significant impacts on visibility and transportation that may evolve under ongoing climate change. This study analyzes the spatial transformation and trends in fog properties in Poland from 1973 to 2020. The research utilises synoptic measurements from IMGW-PIB, the Integrated Surface Database, and long-term emissions data from the Peking University repository. To evaluate the influence of various factors on fog properties, a Random Forest Regressor model was employed. Results indicate regional variation in fog frequency, with higher occurrences (69–77 days/year) at certain stations (Zielona-Góra, Chojnice, Kielce) and lower frequencies in coastal areas (below 40 days/year). The duration of fog events ranges from 3.7 to 6.1 h/day, with visibility between 380 and 590 m. Trends in fog days shifted from a decline of 8.4 days/decade before 1990 to 4.4 days/decade afterwards. While central and northern Poland experienced a reduction in fog days pre-1990, an increase was observed in the southern regions. Post-1990, fog duration decreased significantly (−0.45 h/decade). Meteorological factors were found to influence fog occurrence strongly. Days with low wind speeds (< 3 m/s) showed a moderate correlation (0.47) with annual fog days, while mountainous regions and elevation had strong positive correlations (0.91 and 0.84, respectively). High humidity (100%) correlated moderately (0.42), whereas temperature exhibited a negative correlation (−0.78). The Random Forest model effectively predicted fog days, achieving an R^2 score of 0.64 for stations outside mountainous regions and 0.95 when including all stations, with minimal changes in the root mean square error (12 to 12.5 days/year).

1 | Introduction

Fog is a phenomenon caused by condensed water vapour that is suspended in the atmosphere, close to the surface of the earth. Fog reduces visibility below 1000 m and is greatly influenced by the surroundings, for example topography, water reservoirs, and so forth (Lakra and Avishek 2022). Fog is one of the most frequently occurring hazards (WMO 2010) resulting in huge social and economic complications. Fog conditions often result in reduced visibility, leading to traffic accidents, disruptions in public transportation schedules, and increased travel times. The agricultural sector is another domain significantly affected

by fog, for example, the high relative humidity (RH) associated with fog can increase the risk of plant diseases (Chaloner et al. 2021), affecting the overall agricultural productivity of the country. However, fog can also enhance agricultural productivity as found in (Baguskas et al. 2018). The influence associated with its occurrence depends on its duration and intensity (Shrestha et al. 2022). Furthermore, fog plays a crucial role in the hydrological cycle, impacting regional water resources, agricultural practices, and ecosystems (Bruijnzeel et al. 2006).

(Vautard et al. 2009) showed that in Europe a strong general decline in the frequency of low-visibility phenomena has been

found over the past three decades. Moreover, the results presented strongly suggest that air quality improvement during the past decades has made a large contribution to the increasing visibility trend. In the case of Eastern Europe, observed trends are consistent with the decline of aerosol loads (Markowicz et al. 2019; Markowicz et al. 2022), especially during and after the decline of socialist economies in the late 1980s and early 1990s (Osinski 2004).

Fog usually occurs when the RH has exceeded 100% and the critical supersaturation is reached (Seinfeld and Pandis 2006). Research presented by (Klemm and Lin 2016) focused on urban polluted air masses with RH just below 100%. Results described by (Klemm and Lin 2016) suggested that higher aerosol concentrations lead to an intensification of fog. It was also reported that a 10% change in the aerosol concentration (no changes in composition) had about the same effect on fog as a 0.1°C temperature change. (Klemm and Lin 2016) suggested that the decrease of fog in urban areas is rather correlated with a decrease of the emissions of precursor gases for the formation of small, hygroscopic particles (SO_2 , NO_x) than with the emissions or concentrations of coarse particulate material. However, the urban heat island caused by urbanisation can counteract the effect of aerosol emissions (Yan et al. 2020). The urban heat impact is manifested in sharp urban–rural gradients in surface temperatures and fog thickness (Gautam and Singh 2018) and can influence the occurrence of fog holes and cloud enhancements (Fuchs et al. 2022). Overall, both air quality and climate change can cause changes in fog trends (Yan et al. 2019; Gray et al. 2019).

Poland, situated in Central Europe, is characterised by diverse geographical features, including vast plains, mountain ranges, sea shore, and numerous lakes. These varied landscapes, combined with the country's temperate climate, make Poland susceptible to fog formation under certain weather conditions (Ustrnul et al. 2010). Understanding the mechanisms behind fog formation in Poland requires an analysis of various contributing factors (Ustrnul et al. 2013). These include the influence of geographical features, such as the Baltic Sea, the Sudeten and Carpathian mountain ranges, and the presence of lakes and rivers. Additionally, meteorological factors, such as temperature inversions, air pollution, and humidity levels, play a crucial role in fog formation. Fog in Poland can have diverse characteristics, ranging from light and patchy to dense and persistent, impacting visibility and creating atmospheric conditions that necessitate adaptive strategies.

High-resolution information on fog occurrence in large areas can be obtained from satellite sensors, especially geostationary ones. In the study of (Egli et al. 2017) a baseline climatology of fog and low stratus (FLS) for Europe, based on data recorded from 2006 to 2015 by the Spinning Enhanced Visible and Infrared Imager system (SEVIRI) aboard the Meteosat Second Generation satellites has been created. Trends of SEVIRI derived FLS (h/day) over Poland vary depending on the season (Egli et al. 2017), (Figure 10a–d therein). In winter time FLS trends are strongly negative for all Poland areas (up to -0.25 h/day). For both spring and summer trends vary between 0.10 and -0.10 h/day, depending on the region. Negative trends are observed mainly in northern Poland,

while in southern positive ones. During autumn FLS trends are mostly positive (up to 0.15 h/day). However, when looking into METAR data for single stations (Figure 10e–h) in (Egli et al. 2017) there is much more diversity in FLS values observed. Also, a lot of discrepancies with SEVIRI products are visible (e.g., seaside stations).

There are several types of fog, but the great majority of cases of fog in Poland have a complex origin, which is caused by diverse topography and microclimatic conditions. The most common types of fog are advection and radiation fog. First ones develop after the advection of a warm air mass over colder surfaces, the weather clears up at night, which in consequence leads to heat emission from the ground. The best conditions favouring the formation of fog are found during the cold season (especially at night) when warm and humid air flows from the south and is directed by the lows over the Atlantic. Radiation fog forms when the ground cools rapidly at night through radiative cooling, causing the air just above it to cool as well. As the temperature drops, the air near the surface reaches its dew point, leading to condensation and the formation of fog. Radiation fog typically develops on calm, clear nights with little or no wind. It is most common in valleys or low-lying areas and usually dissipates after sunrise as the ground warms up. A study presented by (Pauli et al. 2020) shows that mean sea level pressure, near-surface wind speed and evapotranspiration are the most important factors that influence FLS occurrence. According to (Ustrnul et al. 2015) the greatest number of days with recorded fog is in October and November; the smallest—from May to July.

(Lorenc 2012) analysed meteorological data from Poland for the short period of 2001–2005. The reported incidence of fog at the analysed stations was very diverse. For instance, surprisingly large decreases in the average number of days with fog were observed at the stations in Opole, Krakow, and Zielona Gora, located in Southern Poland. (Lorenc 2012) suggested that the changes in anthropogenic aerosol emissions, in particular a decrease in the concentration of particulate matter may have a large impact on the reduction in the number of days with fog, for example in Krakow or Opole.

A comprehensive analysis of climate change in Poland, including changes in the frequency of fog occurrence was presented by (Me et al. 2021). The authors analysed data on fog occurrence from 26 Polish meteorological stations for the period 1966–2018. The fog frequency was up to 300 days per year in the high mountains with low annual variability. On the other hand, the lowest number of days with fog (about 28 days) and high annual changes were reported for the Baltic Sea seaside.

The purpose of this paper is to provide a comprehensive overview of the phenomenon of fog in Poland. Our study aims to analyse the spatial changes in fog occurrence in Poland, as well as to answer the question of how trends in fog frequency and occurrence have changed during the last decades (1973–2020) was available. We aim to explore regional variations of fog occurrences within the country and to assess the influence of various factors on fog properties. In conclusion, this paper seeks to study the phenomenon of fog in Poland, providing an understanding of its changes, regional variations, and driving factors.

This knowledge can help improve weather forecasting systems and enhance transportation, aviation, and navigation safety measures.

The paper is divided into several sections. Section 2 outlines the methodology, including a description of the data sources and data processing. Section 3 provides an overview of fog occurrence. Section 4 is dedicated to the study of trends in fog properties. Section 5 includes a description of the station clustering. Next Section 6, presents results of the investigation of fog change due to temp, RH, and PM₁₀ variability, including results of the number of days with fog in a year estimation. In the Discussion and Conclusions, Section 7, the paper is summarised with the highlights of the obtained results.

2 | Data and Methods

2.1 | Data

In this study, we use both observation and numerical simulation data.

2.1.1 | IMGW-PIB

The first dataset used in the presented study is meteorological data from Polish synoptic WMO stations of the Institute of Meteorology and Water Management—National Research Institute (IMGW-PIB). Verified by IMGW-PIB staff meteorological data from year 1960 is available for download at the site (IMGW-PIB [n.d.](#)). Files contain numerous synoptic information for different averaging times (monthly, daily, and hourly data). We used daily averaged data since it provides information on fog duration (occurrence) (h/day).

2.1.2 | NOAA

The Integrated Surface Database (ISD) is a global database that consists of hourly and synoptic surface observations compiled from numerous sources into a single common format and common data model (Smith et al. 2011). ISD includes numerous parameters such as wind speed and direction, wind gust, air temperature, dew point, cloud data, mean sea level pressure, altimeter setting, station pressure, present weather, visibility, precipitation amounts for various periods, snow depth, and various other atmospheric elements as observed by each station. The data files are derived from surface observational data and are stored in ASCII character format. Dataset reaches year 1950 and is accessible via NCEI's Climate Data Online system (NCEI's Climate Data Online system [n.d.](#); National Centers for Environmental Information [n.d.](#)). After downloading files for all Polish stations, we checked the length of the time series. For our studies, we used ISD information on visibility, air temperature, wind speed, and dew point temperature to calculate RH. Visibility data was in the next steps used for checking the number of days with fog (or fog days) in each year. Fog day is defined as a day when visibility below 1 km was recorded, regardless of the number of hours with fog.

2.1.3 | Emissions

As a source of long-term emissions data from the Peking University repository (PKU) was used. The PKU research group produced and provided a series of global emission inventories for several substances, including PM_{2.5}, PM₁₀, BC (Black Carbon) (Wang et al. 2013; Chen et al. 2017) applied a space-for-time substitute method to calculate monthly (or daily) residential fuel consumption and, consequently, monthly emissions of individual pollutants. The intra-annual variations associated with agricultural waste burning, deforestation, and wildfires were obtained directly from the Global Fire Emissions Database (GFED) (van der Werf et al. 2010). For this study the monthly total emissions, by pollutant, with 0.1 by 0.1° spatial resolution was downloaded from the website (Peking University Repository [n.d.](#)). The files contain monthly gridded emission data (1800×3600) provided in the Network Common Data Form (NetCDF). Each file includes 12 monthly datasets for a given year. Global emission inventories cover the period from 1960 to 2014. For this work emission data for 3 substances was acquired: BC, PM₁₀, and PM_{2.5}. The sources of pollutants that were taken into account are coal, oil, gas, waste, biomass, non-combustion processes, and open fires. The total number of sources per pollutant is BC—73 sources, PM_x—80 sources. The detailed sources are listed in the table provided by PKU (PKU [n.d.](#)).

2.2 | Data Processing

For further analysis, we used only stations for which a complete set of data from the years 1973–2020 was available. Such definition of the measurement period ensured data availability from all databases taken into account, as well as allowing us to observe changes resulting from the industrial transformation in Poland that occurred in a few years after 1989 (Osinski 2004). Following our previous studies (Markowicz et al. 2019; Markowicz et al. 2022) as a breakthrough year we picked 1990. This choice is based mostly on a substantial decrease in emissions of pollutants connected to the collapse in the Polish industry (example presented in Figure A1), but also on observed decrease in measured AOD (Markowicz et al. 2022).

All data was carefully checked, cleaned, and then averaged to the monthly and annual means. Although stations with the fullest possible data series were selected, few small data gaps were possible. In those cases, missing data have been filled with climatological means. As a result, we prepared a dataset for 39 stations presented in Figure 1. A List of stations with additional information can be found in Table 1. For trend analysis, only 37 stations were taken into account. Two stations, Kasprowy Wierch (1989 m a.s.l.), and Sniezka (1612 m a.s.l.) were omitted in this part of the analysis because of their specific location. Both are placed in the high mountain area, on the tops of the mountains which results in significant differences in meteorological conditions.

Besides two strictly mountain stations, there are 5 sites located directly by the Baltic Sea. The remaining stations are spread quite evenly through the country in the lowlands and highlands (southern Poland). Most of the measurement sites are placed close to cities.

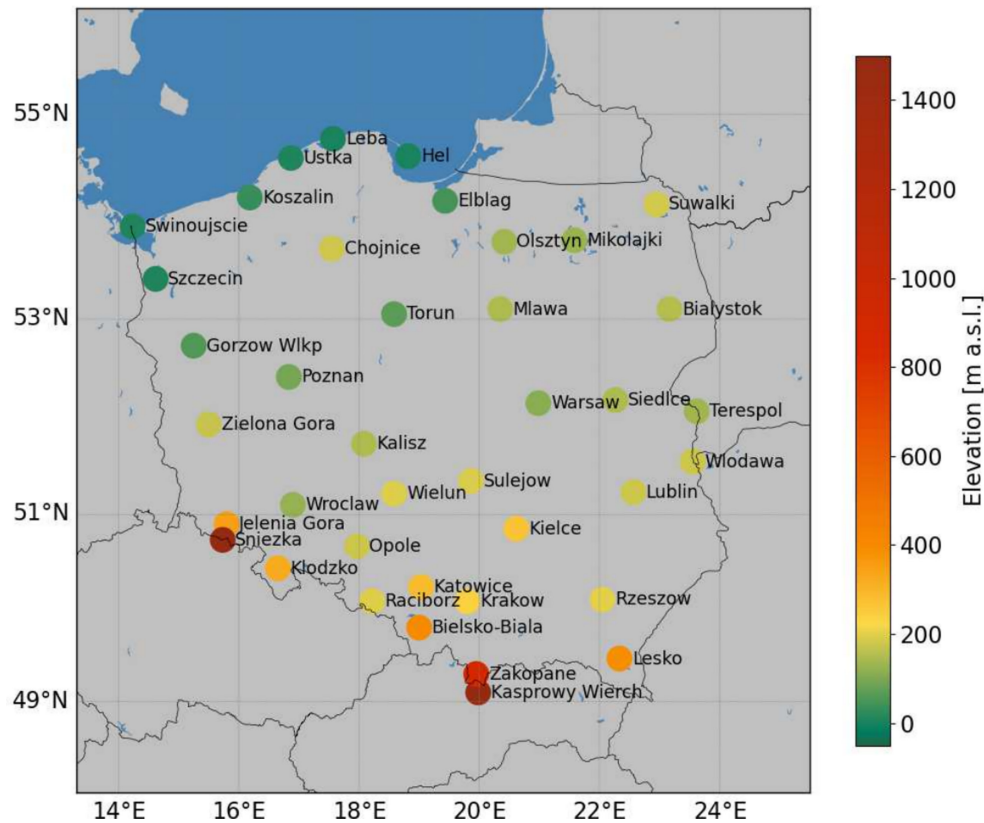


FIGURE 1 | Location, elevation [m a.s.l.] and names of measurement WMO stations used in the analysis. [Colour figure can be viewed at [wileyonlinelibrary.com](https://onlinelibrary.wiley.com)]

2.2.1 | Random Forest Model

To predict the number of days with fog (dependent variable) in a year based on the set of variables we decided to use machine learning methods. As a method, we decided to use the Random Forest Regressor model. Random forests consist of multiple tree predictors, where each tree relies on values from a random vector that is independently sampled and follows the same distribution across all trees in the forest (Cutler et al. 2012). (Breiman 2001) described random forests as effective tools that do not overfit and are accurate classifiers and regressors.

Independent variables that were chosen for this study include annual means of air temperature [°C], site elevation [m a.s.l.], PM₁₀ emission [kg], number of days with RH=100% [days/year], number of days with wind < 3 m/s [days/year], days with favourable conditions (RH=100% and wind < 3 m/s) [days/year], water reservoir influence [none/weak/strong], station type [urban, suburban, background, seaside, mountains], and proximity to the airport [yes/no]. Because of the essential differences between stations located on top of the mountains and the remaining ones, we decided to run calculations for two versions of data sets: mountain stations (Kasprowy Wierch and Sniezka) excluded and included. To prepare data for model building we split our dataset randomly (random_state = 42) into training data (80%) and test data (20%). As a result, there were 1,177 points in the training dataset and 295 points in testing one. For our simulations we used Scikit-Learn Random Forest Regressor and the best hyperparameters were calculated from GridSearchCV

on the grid n_estimators=[1100, 1200, 1300, 1400], max_depth=[10, 20, 30, 40], cv=3. As a result, hyperparameters were set to n_estimators=1100, max_depth=40. The random_state value was set to 42. After fitting the model with training data, the model was run for the test set of data.

3 | Overview of Fog Occurrence

In Figure 2 mean annual cycles of fog occurrence and days with observed fog are presented. Annual changes are similar in both cases. The smallest number of fog cases is recorded in late spring and summer (below 4 days per month), especially in July, when the fog lasts the shortest as well (close to 3 h). Maxima is observed in November when the fog appears on more than 7 days and fog occurrence is close to 7 h. It is consistent with the results presented by (Ustrnul et al. 2010; Skomorowski and Piotrowski 2018).

Below long-term means of fog-related parameters are depicted in the form of maps prepared for Poland territory. In Figure 3 long-term mean of the number of days with fog per year is presented. Two stations that visibly stand out are Kasprowy Wierch and Sniezka (250 and 290 days/year with fog respectively). Both sites are located at the top of the mountains, where the fog is reported as low-level clouds. Other stations with a relatively high number of days with fog are Kielce, Chojnice, and Zielona-Gora (77, 75, and 69 days/year). A lower mean number of days with fog (below 40 days/year) was reported for three sites located at the Baltic Sea: Swinoujscie, Hel, Ustka (24, 30, 30 days/year), and

TABLE 1 | List of measurement stations with additional information.

Station type	Station name	Lon	Lat	Elevation [m a.s.l.]	Airport (y/n)	Water res. influence	Topography
Background	Lesko	22.333	49.467	386	No	None	Hill
	Mikolajki	21.583	53.783	131	No	Strong	
	Rzeszow	22.050	50.100	202	Yes	None	
	Sulejow	19.867	51.350	189	No	Strong	
	Elblag	19.433	54.167	43	No	None	
Mountains	Sniezka	15.733	50.733	1,612	No	None	Peak
	Kasprowy Wierch	19.983	49.100	1,989	No	None	Peak
Seaside	Koszalin	16.183	54.200	34	No	Strong	
	Leba	17.567	54.767	2	No	Strong	
	Swinoujscie	14.233	53.917	5	No	Strong	
	Ustka	16.867	54.583	8	No	Strong	
	Hel	18.817	54.600	3	No	Strong	
Suburban	Gorzow Wlkp	15.250	52.733	56	No	None	
	Jelenia Gora	15.800	50.900	344	No	None	
	Kielce	20.617	50.850	270	No	None	
	Klodzko	16.650	50.433	320	No	None	
	Krakow	19.800	50.083	237	Yes	None	
	Lublin	22.567	51.233	177	Yes	None	
	Mlawa	20.350	53.100	146	No	None	
	Olsztyn	20.417	53.767	135	Yes	None	
	Raciborz	18.217	50.083	193	No	None	
	Siedlce	22.267	52.183	146	No	None	
	Suwalki	22.950	54.133	186	No	None	
	Szczecin	14.617	53.400	7	No	Strong	
	Terespol	23.617	52.067	135	No	Strong	
	Warszawa	20.983	52.150	109	Yes	None	
	Wielun	18.583	51.217	198	No	None	
	Wlodawa	23.550	51.550	175	No	Weak	
	Urban	Wroclaw	16.900	51.100	124	Yes	None
Zielona Gora		15.500	51.933	174	No	None	
Chojnice		17.550	53.700	177	No	Strong	
Bielsko-Biala		19.000	49.800	398	No	None	
Kalisz		18.083	51.733	144	No	None	
Katowice		19.033	50.233	284	Yes	None	
Opole		17.967	50.667	176	No	None	
Poznan		16.833	52.417	92	Yes	None	
Torun		18.583	53.050	70	No	Weak	
Zakopane		19.950	49.300	860	No	None	
	Bialystok	23.167	53.100	151	Yes	None	

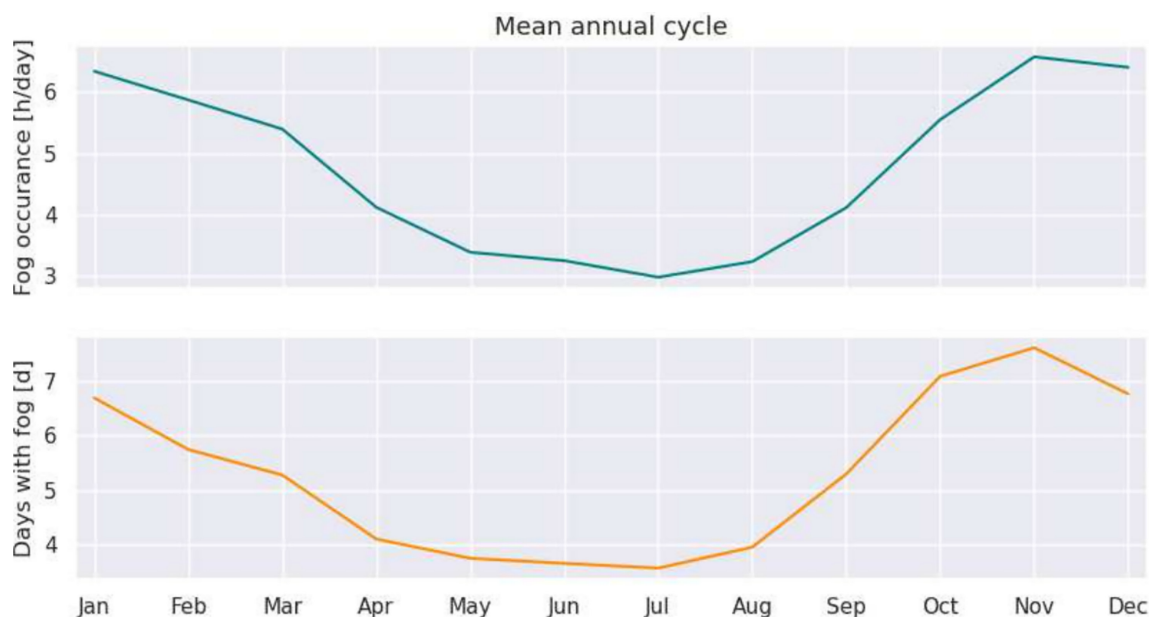


FIGURE 2 | Mean annual cycles of the fog occurrence [h/day] (upper) and days with fog [days] (lower), Poland area for years 1973–2020. Data was averaged for all stations. [Colour figure can be viewed at [wileyonlinelibrary.com](https://onlinelibrary.wiley.com)]

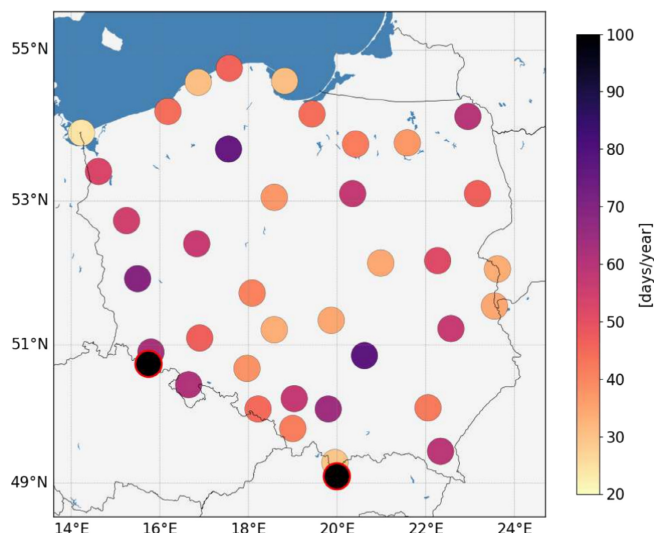


FIGURE 3 | Long-term (1973–2020) mean of number of days with fog per year. The values at the mountain stations (marked with a red circle) are off the scale. [Colour figure can be viewed at [wileyonlinelibrary.com](https://onlinelibrary.wiley.com)]

for Zakopane (29 days/year), which is a small city near (approximate 8 km) Kasprowy Wierch mountain. In general, the spatial distribution of fog days is complex and from station data, a clear dependency on geography is not visible in the context of this study.

In Figure 4 the mean number of days with conditions favouring fog occurrence is plotted. Favourable conditions were set as RH of 100%, and wind speed < 3 m/s. The spatial distribution of this parameter is complicated and shows different meteorological conditions at WMO stations. There are four stations where the favourable conditions defined above are observed during more than 120 days/year: Krakow, Warszawa, Poznan, and Szczecin

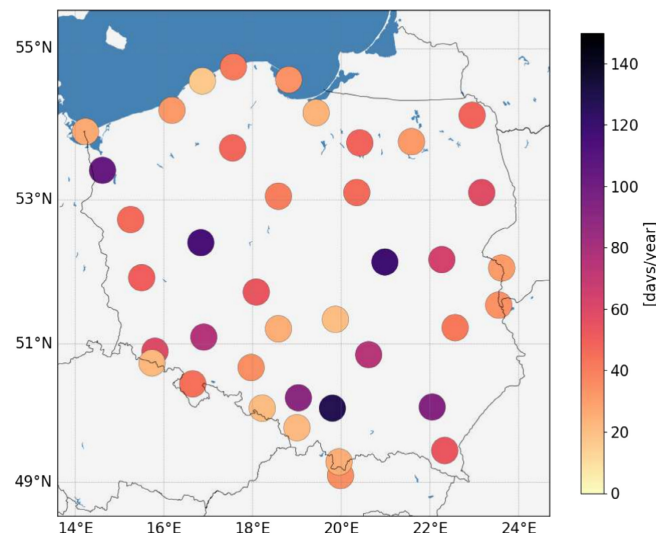


FIGURE 4 | Mean number of days with favourable conditions [days/year]: RH = 100%, wind speed < 3 m/s. [Colour figure can be viewed at [wileyonlinelibrary.com](https://onlinelibrary.wiley.com)]

(128, 118, 115, and 103 days/year). The listed measurement sites are located in different parts of Poland, however, all are in the proximity of large cities. A relatively high number of days with favourable conditions is also reported for Rzeszow and Katowice (90 and 93 days/year), as well as for Wroclaw and Kielce (76 and 74 days/year). The lowest value was reported for Ustka (only 17 days/year). Only about 20–25 days/year with conditions favourable for fog formation occurs in such sites as Sulejow, Bielsko-Biala, Raciborz, Sniezka, Elblag, Wielun, Swinoujscie, Zakopane.

To check how often the conditions formulated above translate into the actual fog formation we analysed the percent of days when fog occurred while favourable conditions were observed (Figure 5 and Figure 6). For four stations (Sniezka, Kielce,

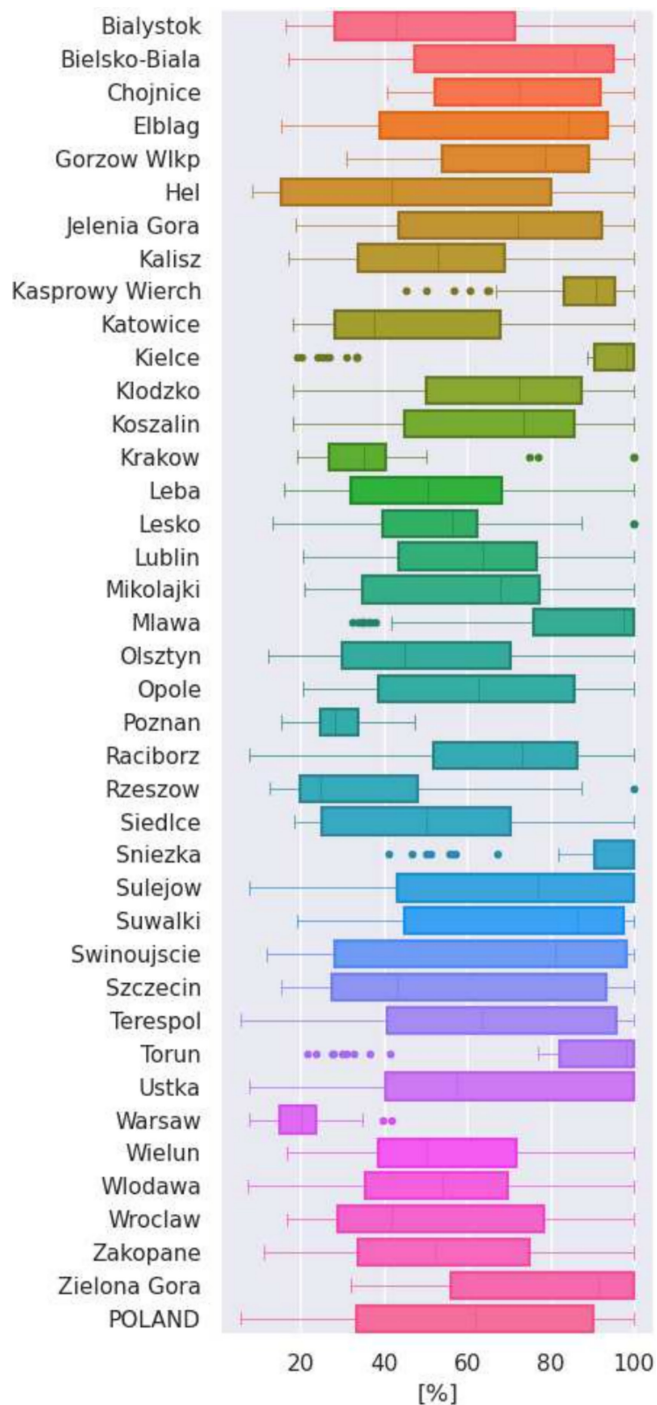


FIGURE 5 | Percent of days when fog occurred while favourable conditions were observed [%]. Favourable conditions: RH = 100%, wind speed < 3 m/s. [Colour figure can be viewed at [wileyonlinelibrary.com](https://onlinelibrary.com)] [19]

Torun, and Mlawa), the median was near 100%, while for the next two stations (Kasprowy Wierch and Zielona Gora), it was close to 90%. On the opposite lowest median was reported for Warszawa, Rzeszow, Poznan, and Krakow (20%–35%).

The interquartile range (IQR) that measures the spread of the middle 50% of the data varied significantly depending on the measurement station. The lowest IQR was 10%–15% for Warszawa, Poznan, Sniezka, Kielce, Krakow, and Kasprowy

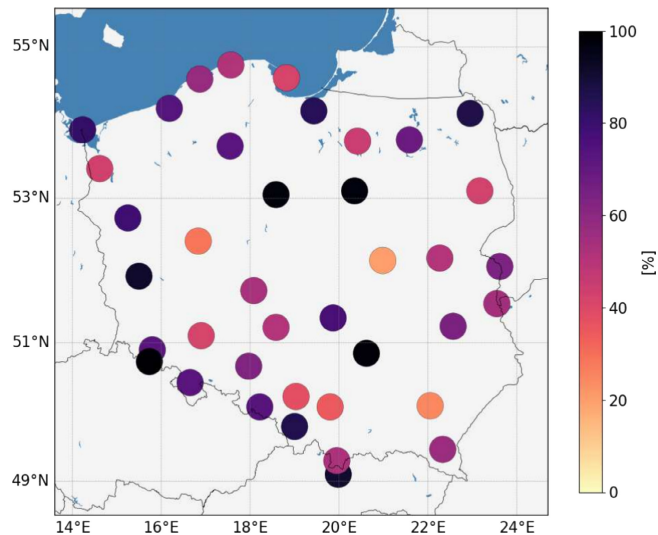


FIGURE 6 | Map of the percent of days when fog occurred while favourable conditions were observed [%]. Favourable conditions: RH = 100%, wind speed < 3 m/s. [Colour figure can be viewed at [wileyonlinelibrary.com](https://onlinelibrary.com)] [20]

Wierch. There were quite a few sites with significant data spread, such as Swinoujscie, Szczecin, Hel, Ustka (seaside). Extremely different values of such parameters can be probably explained by local conditions. It is well-known that fog (especially radiation fog) is sensitive to local conditions, including orography, distance to water reservoirs and so on (Pérez-Díaz et al. 2017). The median for the whole Poland area was slightly above 60% and the interquartile range was between 30% and 90%.

The highest mean number of hours with fog during the day (Figure 7) was observed at the Kasprowy Wierch (13 h) and Sniezka peaks (16 h), which are most likely caused by the misclassification of clouds as fog events. In the rest of the country, the number of fog hours during the day varies between 3.7 and 6.1 h. The highest fog occurrence was reported in Chojnice, Bielsko-Biala, Raciborz, Zielona Gora, and Suwalki (around 6 h). The lower number of fog hours (< 4 h), on the other hand, is observed in Katowice, Koszalin, Warsaw, Lesko, Rzeszow, Wroclaw, and Leba.

Mean visibility in the fog [m] was presented in Figure 8. Extremely dense fogs (clouds) were usually observed at the mountain stations, Kasprowy Wierch (30 m) and Sniezka (100 m). Except for these two sites, the mean visibility in fog is rather small and changes from 383 to 589 m. The lowest visibility (< 400 m) is observed in Gorzow and Jelenia Gora, and the highest (> 550 m) in Bialystok, Koszalin, and Swinoujscie.

4 | Trends in Fog Properties

Below trend analysis of the fog-related parameters is presented and the changes connected to the industrial transformation are described. To analyse the impact of the industrial transformation in Poland on fog properties, the dataset was split into two parts 1973–1989 and 1990–2020 (details in Section 2.2).

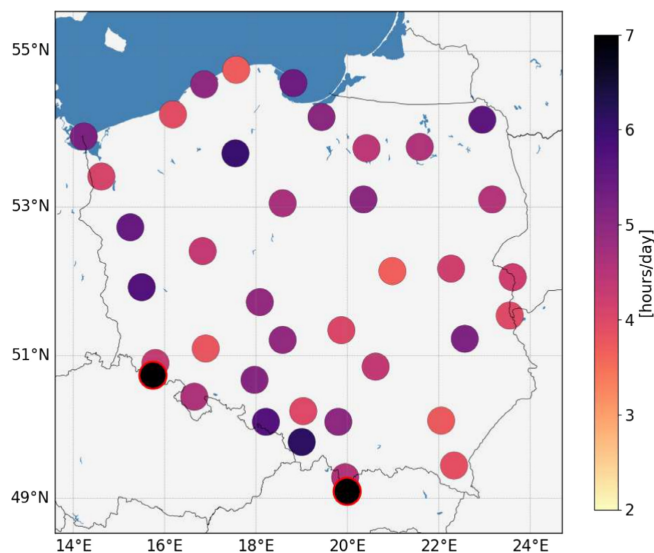


FIGURE 7 | Mean number of hours with fog during the day [h] for years 1973–2020. The values at the mountain stations (marked with a red circle) are off the scale. [Colour figure can be viewed at [wileyonlinelibrary.com](https://onlinelibrary.wiley.com)]

The annual number of fog days (Figure 9) decreased in most central and northern stations and increased in southern Poland. For the period before 1990 trends varied between -2.8% and 11.6% with the mean value of 2.0% . After 1990 the mean trend for Poland is 0.8% , and mean values for stations are from -1.5% to 4.0% (Table 2). Due to high inter-year variability for many stations (especially in Central Poland), trends are not statistically significant.

On most of the stations trends of the number of hours with fog during the day are negative (Figure 10) with the mean for Poland equal -0.15 [h/decade] before 1990 and -0.45 [h/decade] after 1990 (Table 2). For several stations, we observe positive trends for the period before 1990, for example Raciborz, Szczecin, Hel, Koszalin, Warszawa, Kalisz. After 1990 only trends for two stations, Rzeszow and Elblaga, are slightly positive/close to zero.

The mean trend of the visibility in fog for Poland was $+33$ [m/decade] for the period before 1990 and varied between -56 and $+146$ [m/decade] depending on the station (Table 2). After 1990 visibility changed by -6.4 [m/decades], with trends between -64 to $+60$ [m/decades]. Visibility in fog [m/decades] is constantly increasing in Hel, Sulejow, and Chojnice, and decreasing in Ustka, Leba, Koszalin, Jelenia Gora (Figure 11). The positive trends before 1990 and negative ones after 1990 are observed for, among others, Suwalki, Terespol, Lesko, Raciborz, Torun.

5 | Stations Clustering

All stations were split into different groups (types), based on their location (Table 1). Two types of sites were selected due to special geographical conditions: seaside and mountain stations. Considering proximity to a large city we distinguished another three types of stations: urban, suburban, and background.

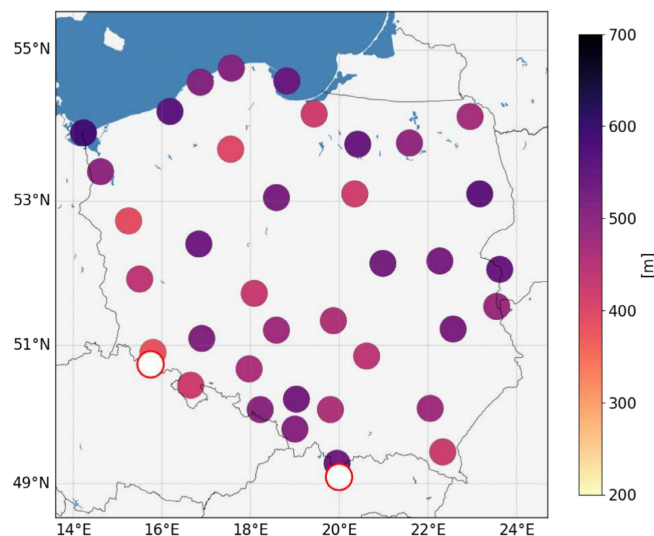


FIGURE 8 | Mean visibility in the fog [m] for years 1973–2020. The values at the mountain stations (marked with a red circle) are off the scale. [Colour figure can be viewed at [wileyonlinelibrary.com](https://onlinelibrary.wiley.com)]

Additional information includes site elevation [m a.s.l.], water reservoir influence [none/weak/strong], proximity to the airport [yes/no], and notes on topography. In the case of water influence, we designate strong influence for sites located within 1 km of a reservoir. Weak influence is assigned to sites near the water body (< 1 km) but situated at a higher elevation.

In Table 2 mean trends of the number of days with fog, number of hours with fog, and visibility in fog for different station types are presented. For the background stations, statistically significant and positive trends were obtained in the case of the fog days ($+6.2\%$ before 1990 and $+2.0\%$ after 1990). The hours with fog are decreasing in both periods, but the trends are not significant. The mean visibility in fog increased before 1990 and slightly decreased later. For both mountain stations, positive and significant trends in days with fog and mean visibility are observed. Similarly to the background stations, the reduction of hours with fog before and after 1990 is measured at mountain sites. Fog temporal variability for the seaside stations is small and not statistically significant. In the case of suburban and urban sites trends are not significant but the pattern is similar to the background site. Increase of the days with fog (larger before 1990), a reduction of hours with fog, an increase in fog visibility before 1990, and a decrease after 1990.

6 | Identifying Factors Influencing the Characteristics of Fog in Poland

In order to attempt an assessment of the factors that play an important role in fog processes we decided to estimate the number of days with fog in a year based on the set of variables with the use of the Random Forest Regressor model.

In Figures 12 and 13 heat maps of the Pearson correlation coefficient of the variables are presented for the dataset with mountain stations excluded and included respectively. In the first

version of the dataset, the number of days with fog variable is statistically correlated with meteorological conditions, especially with the number of days with wind < 3 m/s (0.47). The positive but relatively low correlation coefficient (0.32) is obtained for the suburban type of station. On the other hand, a negative correlation coefficient was shown for parameters related to the presence of water reservoirs.

Including mountain stations (Figure 13) caused substantial changes in results. The biggest change concerned a higher correlation coefficient of the number of days with fog with mountain type of stations and elevation (0.91 and 0.84). The correlation coefficient of the number of days with fog and the number of days with RH=100% is 0.42. At the same time, air temperature is significantly negatively correlated (-0.78) with the number of days with fog.

After training the model, it was run for the test set of data. Results of these calculations are presented in Figure 14. In general number of days with fog is predicted with relatively good

accuracy, however model tends to underestimate higher values and overestimates lower ones. A linear fit is significantly better when mountain stations are taken into account (14 b), which is caused by the presence of the data points in the upper range of values.

R^2 is a statistical measure that indicates how much of the variation of a dependent variable is explained by an independent variable in a regression model. The R^2 score for the testing set for the case when mountain stations were excluded was 0.64 while including all stations resulted in 0.95. However, the Root Mean Square Error (RMSE) changed only from 12 to 12.5 [days/year].

In Figure 15 model features (variables) importance are presented for two cases: (a) mountain stations excluded, (b) mountain stations included. The importance parameter indicates how much each feature contributes to the model prediction. It is a measure of how much removing a variable decreases accuracy, and vice

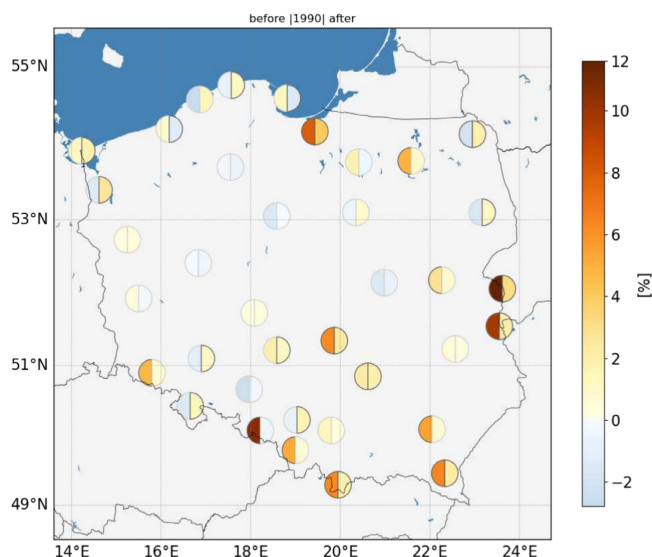


FIGURE 9 | Relative trends [%] of the number of fog days in two periods: 1973–1989 (left half of the circle) and 1990–2020 (right half of the circle). Statistically significant trends are marked with a dark grey border. [Colour figure can be viewed at [wileyonlinelibrary.com](https://onlinelibrary.wiley.com)]

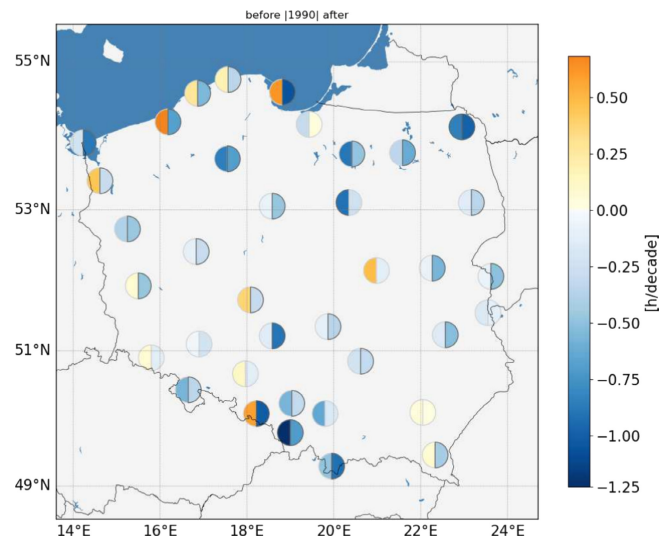


FIGURE 10 | Trend of the number of hours with fog during the day [h/decade] in two periods: 1973–1989 (left half of the circle) and 1990–2020 (right half of the circle). Statistically significant trends are marked with a dark grey border. [Colour figure can be viewed at [wileyonlinelibrary.com](https://onlinelibrary.wiley.com)]

TABLE 2 | Mean trends for different station types for days with fog, hours with fog, and fog visibility before and after 1990.

Station type	Days with fog [%]		Hours with fog [h/decade]		Vis in fog [m/decade]	
	Before	After	Before	After	Before	After
Background	+6.18 (1.17)	+2.02 (1.39)	-0.12 (0.19)	-0.27 (0.28)	+63.0 (42.34)	-8.47 (27.38)
Mountains	+2.84 (2.42)	+0.11 (0.01)	-0.7 (0.2)	-0.16 (0.24)	+38.61 (42.53)	+16.08 (9.86)
Seaside	-0.08 (1.72)	+0.3 (1.58)	+0.31 (0.37)	-0.7 (0.27)	+14.65 (48.16)	-11.82 (49.44)
Suburban	+2.07 (4.19)	+0.83 (1.11)	-0.23 (0.46)	-0.45 (0.28)	+29.9 (51.02)	-5.26 (29.75)
Urban	+0.61 (3.25)	+0.53 (0.85)	-0.26 (0.49)	-0.44 (0.26)	+32.9 (63.14)	-4.33 (23.74)
POLAND	+2.06 (3.77)	+0.82 (1.2)	-0.18 (0.46)	-0.44 (0.29)	+33.25 (51.16)	-5.23 (29.88)
Mountains excluded	+2.02 (3.84)	+0.85 (1.22)	-0.15 (3.84)	-0.46 (0.29)	+32.96 (52.06)	-6.38 (30.22)

Note: In brackets, standard deviations are given.

versa—by how much including a variable increases accuracy. For this study, we calculate feature importance in two ways: based on the mean decrease in impurity (the built-in Scikit-Learn *feature_importances_* method, Figure 15a) and permutation method (*permutation_importance_*, Figure 15b). Impurity-based feature importances can be misleading for high cardinality features (many unique values) (Pedregosa et al. 2011). Permutation feature importance overcomes limitations of the impurity-based feature importance: they do not have a bias toward high-cardinality features and can be computed on a left-out test set (Pedregosa et al. 2011).

For simulation with mountain station included the most important features according to the impurity-based measure are air temperature (0.3), elevation (0.28), and mountain type of station (0.28). The lower influence has meteorological conditions such as RH and low wind speed (0.2–0.5). Other variables turned out to be almost irrelevant (Figure 15a). Results from permutation feature importance are similar in quality, but quantitative differences are visible (Figure 15b). The importance of the air temperature, elevation, and mountain type of station is a bit lower than in the previous case. At the same time, the contribution of other variables is higher.

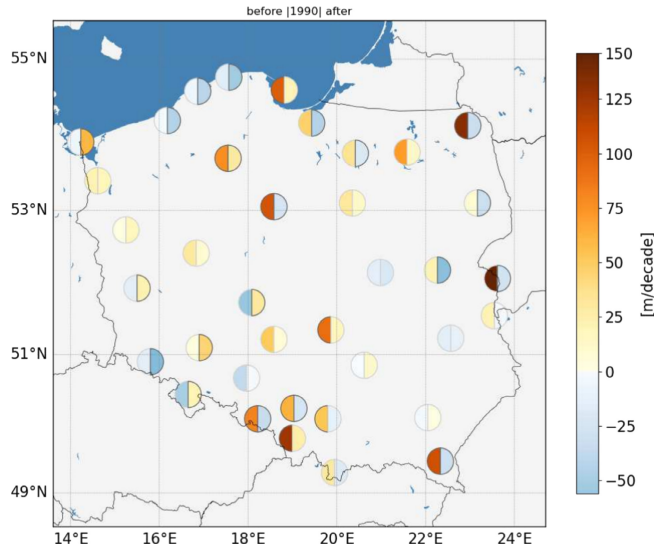


FIGURE 11 | Trend of the visibility in fog in two periods: 1973–1989 (left half of the circle) and 1990–2020 (right half of the circle). Statistically significant trends are marked with a dark grey border. [Colour figure can be viewed at [wileyonlinelibrary.com](https://onlinelibrary.wiley.com)]

When Kasprowy Wierch and Sniezka stations were removed from the dataset features that have the highest impact on model results changed significantly. When impurity was taken into account the most important parameter (0.3) turned out to be the number of days with low wind speed (< 3 m/s) (Figure 15a). Lower importance was reported for elevation, PM₁₀ emissions, number of days with RH = 100, and number of days with favourable conditions (all in the range of 0.12–0.14). Other parameters that only slightly influence calculations can be connected to the station type and water reservoirs (below 0.1). For the permutation-based importance (Figure 15b), the number of days with low wind speed (< 3 m/s) has even more (> 0.4) influence on model results. A similar change can be observed for elevation (increase to > 0.2).

7 | Discussion and Conclusions

This study focuses on the spatial and temporal variability of fog properties in Poland. The analysis is grounded in synoptic observations (IMGW-PIB, NOAA) and emission data (PKU inventory) spanning the years 1973–2020. For this research, 39

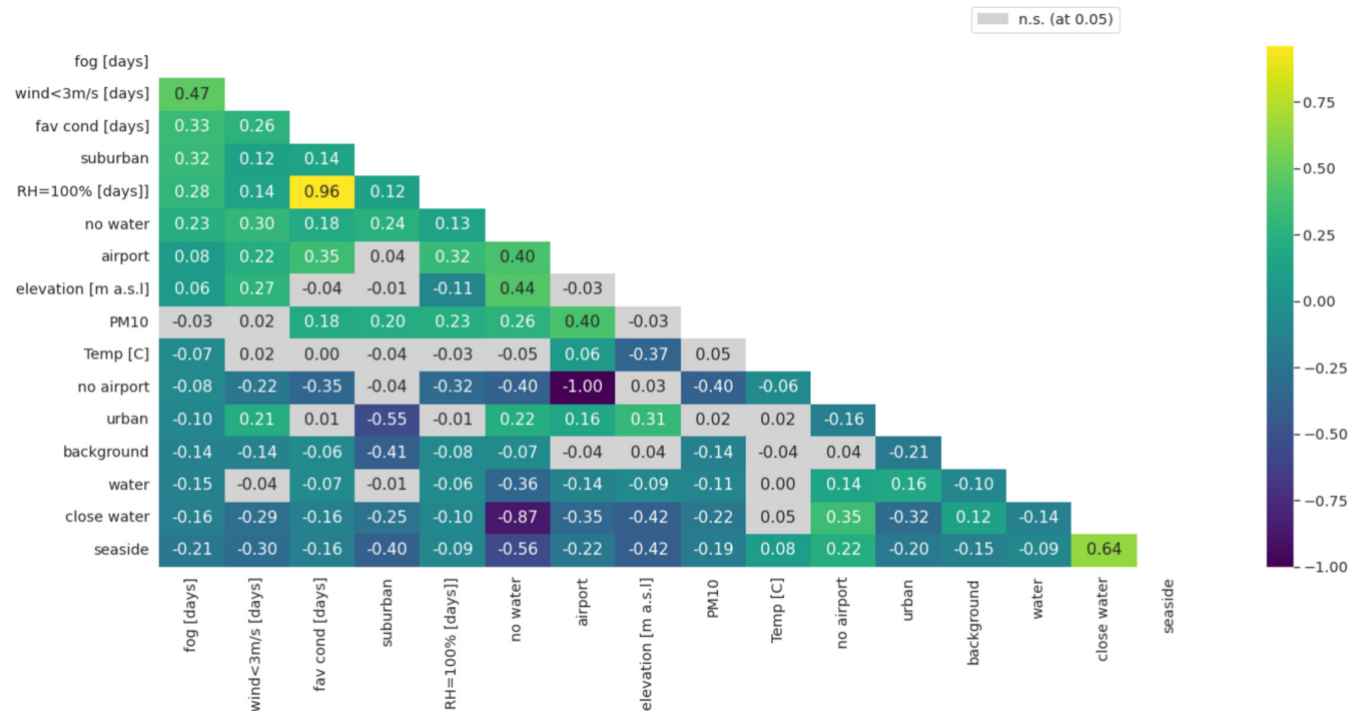


FIGURE 12 | Heat map of the correlation of the variables (mountain stations excluded). Correlations marked with light grey colour are statistically not significant. [Colour figure can be viewed at [wileyonlinelibrary.com](https://onlinelibrary.wiley.com)]

stations with complete data series were selected and categorised into five types: background, mountains, seaside, suburban, and urban.

Due to different micrometeorological conditions, the long-term mean of the number of days with fog spatial distribution is complex and varies from a relatively high number in Kielce, Chojnice, and Zielona-Gora (77, 75, 69 days/year), to a lower mean number at the seaside (below 40 days/year). This can be explained by the prevalence of advection fog at seaside stations (Skomorowski and Piotrowski 2018; Trzeciak 1992), while over land, particularly in terrain depressions, radiation fog is also developed. The annual number of fog days decreased in most central and northern stations while it increased in the southern region of Poland, which is mostly a highland-mountainous area. Due to their complex nature, temporal and spatial fluctuations of fog in southern Poland have been analysed many times in scientific studies (Blas et al. 2002; Blas and Sobik 2004; Hess 1965; Wrzesinsky and Klemm 2000; Zarnowiecki 2000; Wypych 2003; Lupikaszka and Niedzwiedz 2016). In general, the minimum number of fogs occurred during the summer months and the maximum number of fogs was observed in October and November. As reported by (Lorenc 2012) the highest number of days with fog for the years 2001–2005 was observed in Chojnice and Kielce, whilst the smallest number was reported for seaside stations. These results are consistent with our findings despite different periods of interest.

For most stations (excluding mountains), fog occurrence varies between 3.7 and 6.1 h, and the mean visibility in fog is rather small and changes from approx. 380 to 590 m. Analysis of synoptic data from 8 stations located at the largest airports in Poland, based on the METAR (Meteorological Aerodrome Report) conducted by Skomorowski (Skomorowski and Piotrowski 2018)

showed that fog occurrence in most cases did not exceed 3 h for all stations and, fog most often limits the horizontal visibility to 500 m.

Long-term variability of fog phenomena in Poland shows a positive trend of the number of days before (+2.0%/decade) and after 1990 (+0.8%). Trend analysis showed a decrease in the number of days with fog in the west and central part of the country and an increase in the east of Poland. It is important to remember that fog is a phenomenon strongly determined by local conditions, which are strictly connected to the station location. For example, changes in the number of days with fog in Kielce are mainly due to the relocation of the meteorological station to the vicinity of a water reservoir and a river as reported by (Lorenc 2012).

Trends of the mean number of hours with fog during the day are mostly negative with the mean for Poland equal to -0.15 [h/decade] before 1990 and -0.45 [h/decade] after 1990. The trend of the visibility in fog for the period before 1990 varied between -56 and $+146$ [m/decade] with a mean of $+33$ [m/decade]. After 1990 visibility changed by -6.4 [m/decade], with trends between -64 and $+60$ [m/decade]. However, it should be noted that calculated trends are statistically significant only for part of the measurement sites, mainly background and mountain types.

Fog phenomena can be theoretically reported during intensive aerosol episodes below saturated conditions ($RH < 100\%$) (see Appendix A). Figure 16 shows the relation between threshold PM_{10} mass concentration at dry conditions (which reduces visibility to 1 km) as a function of RH. For the $RH = 80\%$, the 1 km visibility can be observed when PM_{10} is close to $500 \mu\text{g}/\text{m}^3$. For upper RH the PM_{10} threshold is moving toward lower values

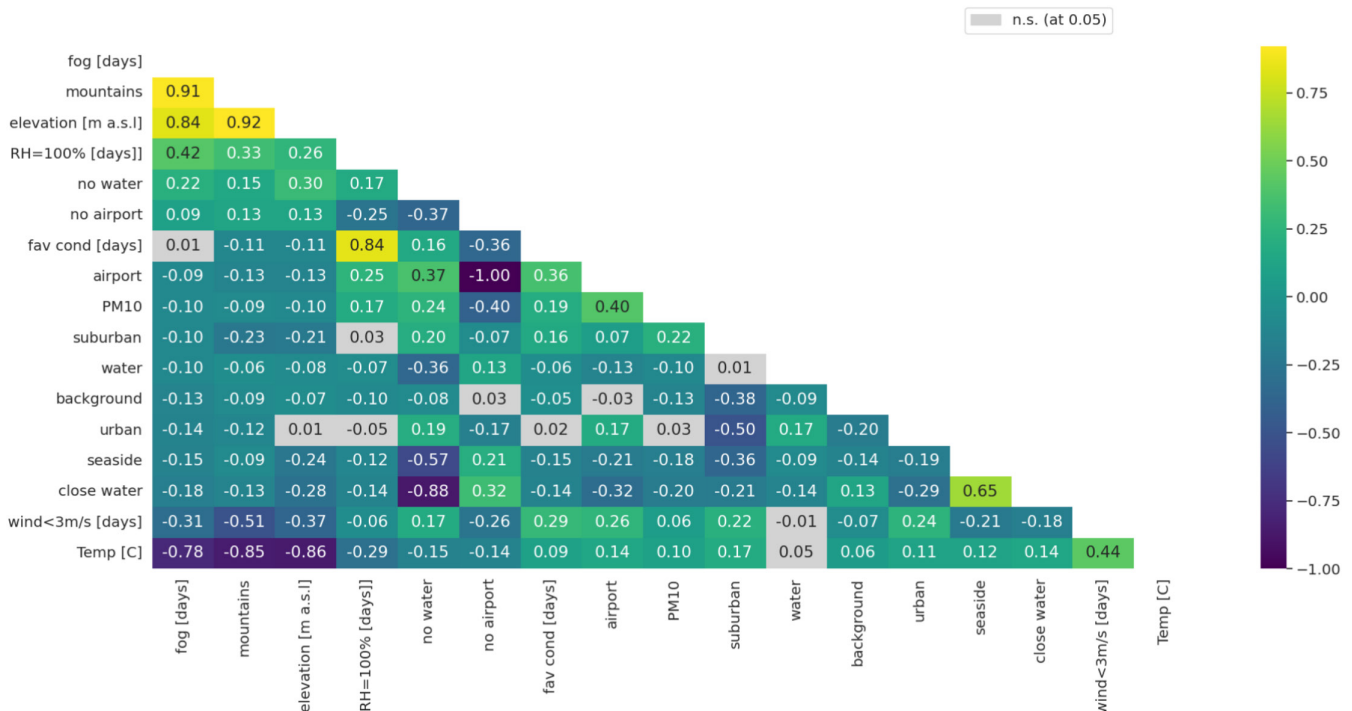


FIGURE 13 | Heat map of the correlation of the variables (mountain stations included). Correlations marked with light grey colour are statistically not significant. [Colour figure can be viewed at [wileyonlinelibrary.com](https://onlinelibrary.wiley.com)]

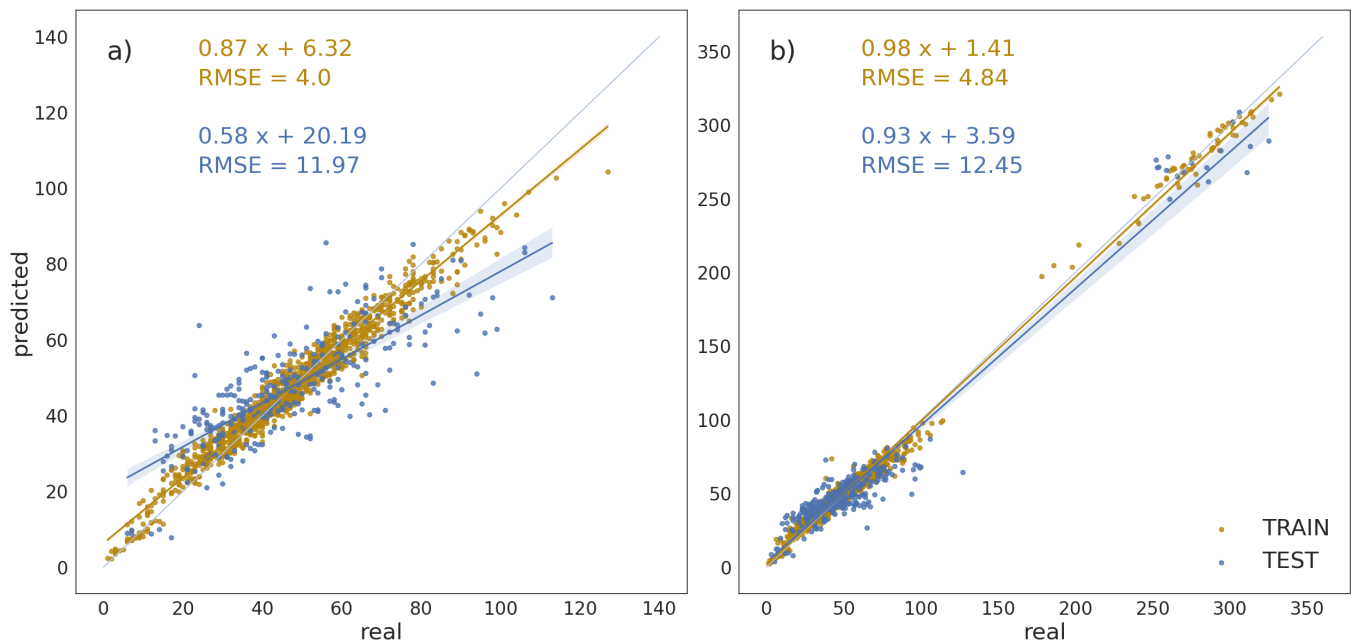


FIGURE 14 | Comparison of the model results (predicted) with the test (real) and training data: (a) mountain stations excluded, (b) mountain stations included. [Colour figure can be viewed at [wileyonlinelibrary.com](https://onlinelibrary.wiley.com)]

(due to hygroscopic effect). At 90% it is about $300 \mu\text{g}/\text{m}^3$, at 95% close to $200 \mu\text{g}/\text{m}^3$. Such levels of PM_{10} are observed in Poland, especially in megacities and small valley villages (Wielgosinski and Czerwinska 2020; Reizer and Juda-Rezler 2016).

Because a significant reduction of emissions after 1990 is noted we can expect a decline in the level of aerosol concentration during smog episodes, which can impact the reported fog phenomena. An increase in fog visibility before 1990 and a decrease later can be probably explained by aerosol changes. Reduced visibility during fog coincides with aerosol decline because visibility is higher during smog conditions than during fog (cloud condensation nuclei activation) (Vautard et al. 2009). Also, for more polluted days the surface solar radiation and air temperature are lower during the daytime, thereby causing longer duration and later dissipation of fog (Li et al. 2000; Shi et al. 2008). Since temperature contributes to the current fog occurrence, another possible explanation for reducing the hours where fog occurs is a positive trend of the air temperature, which for the last 4 decades in Poland is close to $+0.5^\circ\text{C}/\text{decade}$ (Markowicz et al. 2023) and a negative trend of RH (see Figure A2). In the warmer and drier (RH) climate, fog starts to develop later and disappears earlier. Changes in circulation, such as an increase in the number of days with low wind speeds, are likely the cause of the increasing frequency of fog (see Figure 9). On the other hand, lower RH is a factor in reducing the number of fog hours (Figure 10).

The impact of aerosols on fog properties is difficult to resolve in this study, while data on PM_{10} were not available before 1990. In addition, due to different fog types (i.e., radiation, advection, frontal), the variability of fog parameters is complicated when the climate is warming and air quality is improved (Lakra and Avishek 2022). In central Europe, radiation fog is the most frequent fog type especially prevalent during autumn and winter (Egli et al. 2018). This type of fog forms due to radiative cooling at the surface under clear skies typically encountered during anticyclonic conditions (Gultepe et al. 2007).

Therefore, the frequency of radiation fog formation is more sensitive to a number of days with low wind speed (small pressure gradient), clear sky, and a stable boundary layer (Pérez-Díaz et al. 2017) than to mean temperature changes. The number of days with radiation fog favourable conditions (wind speed $< 3 \text{ m/s}$ and $\text{RH} = 100\%$) decreased before 1990 and increased after 1990 (Table A1). Also, before 1990 the reduction of mean RH and number of days with $\text{RH} = 100\%$ is observed. In both periods the number of days with wind less than 3 m/s is increased. Results presented in Figure 5 suggest that it is possible that even when $\text{RH} = 100\%$ there was no fog observed, which could be true for prolonged drizzle. Also, fog can occur in two cases when described above favourable conditions are not fulfilled, heavy smog condition with $\text{RH} < 100\%$ or advection fog with wind speed $> 3 \text{ m/s}$. Advection and frontal fog formation are attributed to synoptic-scale circulation, with the former resulting from alterations in moisture transport over cooler surfaces and the latter from frontal zones. (Petrou et al. 2022) report that the long-term change in frontal passages in central Europe is negligible, while a significant increase in warm, wet, and dry air masses is observed.

An investigation of the fog occurrence in relation to the meteorological conditions favouring its formation (temperature, RH, wind speed) and PM_{10} variability was presented in light of results from the correlation analysis. If mountain stations are excluded, the number of days with fog is moderately correlated with meteorological conditions, especially with the number of days with wind $< 3 \text{ m/s}$ (0.47). A negative correlation coefficient was shown for parameters related to the presence of water reservoirs. The inclusion of the mountain stations results in a high correlation coefficient of the number of days with fog with mountain type of stations and elevation (0.91 and 0.84). A correlation coefficient of 0.42 was obtained for the number of days with $\text{RH} = 100\%$. At the same time, temperature is significantly negatively correlated (-0.78) with the number of days with fog.

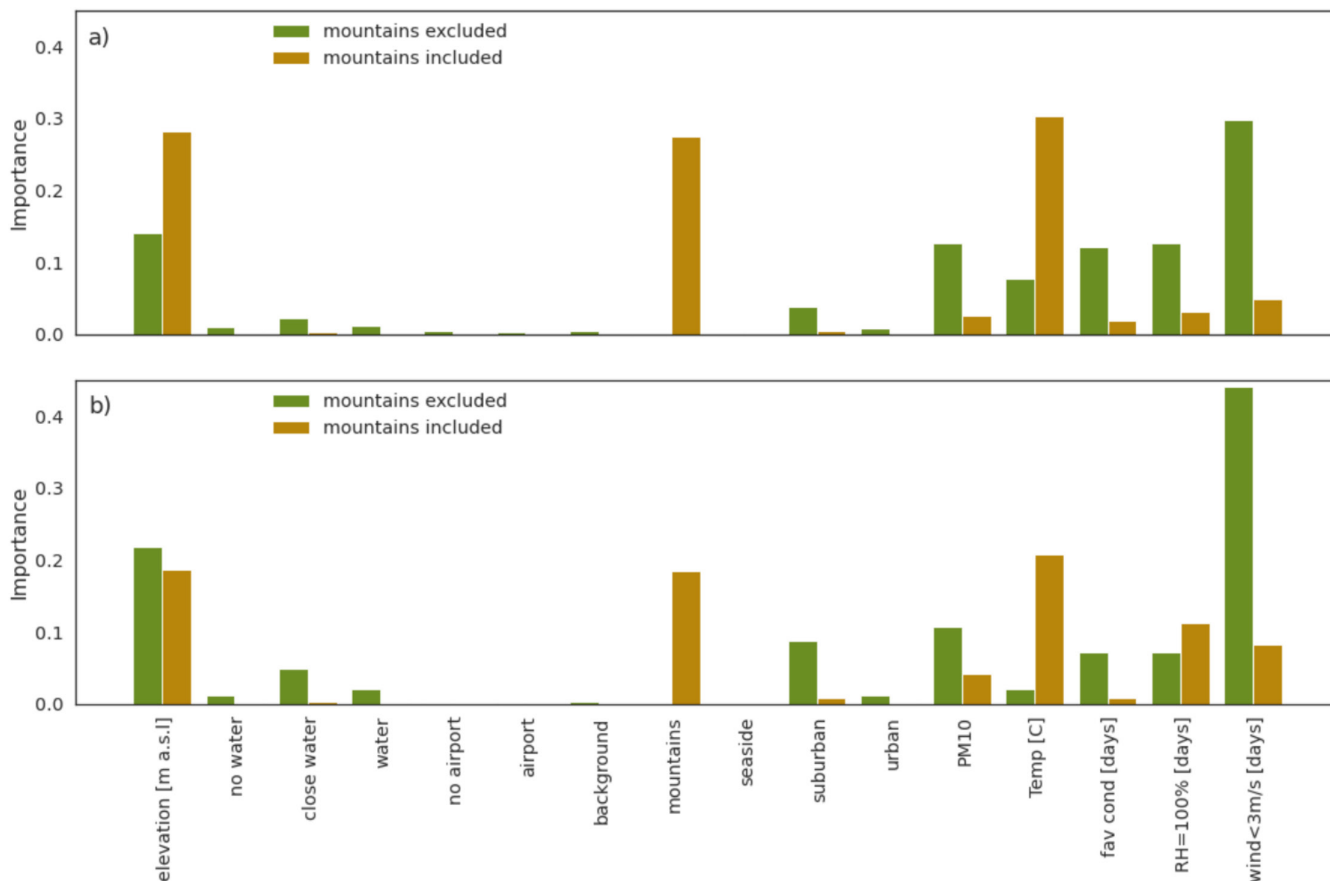


FIGURE 15 | Variables contribution to the model prediction: (a) Feature importance based on the mean decrease in impurity, and (b) Permutation feature importance, calculated for two cases: Mountain stations excluded and mountain stations included. [Colour figure can be viewed at [wileyonlinelibrary.com](https://onlinelibrary.wiley.com)]

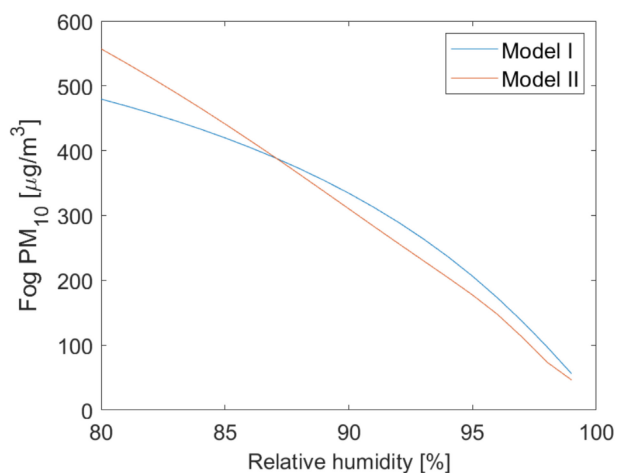


FIGURE 16 | PM_{10} mass concentration corresponding to the visibility of 1 km as a function of the relative humidity. The blue line corresponds to the more sophisticated model (model I) while the red line to the simplified model (model II). [Colour figure can be viewed at [wileyonlinelibrary.com](https://onlinelibrary.wiley.com)]

The number of days with fog in a year was forecast based on the set of variables with the Random Forest Regressor model. The R^2 score for the testing set for the case when mountain stations were excluded was 0.64 while including all stations resulted in 0.95. However, the Root-Mean-Square Error (RMSE) changed

only from 12 to 12.5 days. A similar topic has been raised by (Pauli et al. 2020), where FLS [hours/day] has been predicted with the use of gradient boosting regression trees and satellite data (Egli et al. 2018). Despite differences in both time resolution and source data, the obtained results were similar to ours, with R^2 values between 0.6 and 0.94, highest in winter and lowest in the full-year run. (Pauli et al. 2020) reported that the most important factors were sea level pressure, near-surface wind speed and evapotranspiration, while in our study temperature, elevation and days with low wind speed are usually key factors.

The issue we have presented is very broad, and further exploration of the topic is certainly needed. It would be valuable to analyse the issue by considering both radiation and advection fogs, based on ground data, and incorporating satellite data into the analysis. Additionally, an important aspect to investigate would be identifying cases of misclassification of smog as fog. Further insights could come from validating a theoretical model of fog-aerosol interactions. Moreover, analysing trends related to fog-aerosol interaction in the context of climate change would be particularly interesting.

Author Contributions

Olga Zawadzka-Manko: writing – original draft, visualization, formal analysis, data curation, writing – review and editing, validation, methodology, software, conceptualization. **Krzysztof M. Markowicz:**

writing – review and editing, funding acquisition, conceptualization, methodology.

Acknowledgements

This research was carried out within Polish Grant No. 2017/27/B/ST10/00549 of the National Science Centre coordinated by the Institute of Geophysics, Faculty of Physics, University of Warsaw. One of the sources of the data is the Institute of Meteorology and Water Management—National Research Institute. Data from the Institute of Meteorology and Water Management—National Research Institute have been processed.

Conflicts of Interest

The authors declare no conflicts of interest.

Data Availability Statement

The data that support the findings of this study were derived from the following resources available in the public domain: IMGW-PIB, https://danepubliczne.imgw.pl/data/dane_pomiarowo_obserwacyjne/dane_meteorologiczne/dobowe/-NOAA ISD, <https://www.ncei.noaa.gov/pub/data/noaa/> PKU emission data are available from the corresponding author upon request.

References

- Baguskas, S. A., R. E. S. Clemesha, and M. E. Loik. 2018. “Coastal Low Cloudiness and Fog Enhance Crop Water Use Efficiency in a California Agricultural System.” *Agricultural and Forest Meteorology* 252: 109–120.
- Blas, M., and M. Sobik. 2004. “The Distribution of Fog Frequency in the Carpathians.” *Geographia Polonica* 77: 19–34.
- Blas, M., M. Sobik, F. Quiel, and P. Netzel. 2002. “Temporal and Spatial Variations of Fog in the Western Sudety Mts. Poland.” *Atmospheric Research* 63: 19–28.
- Bohren, C. F., and D. R. Huffman. 1983. *Absorption and Scattering of Light by Small Particles*. A Wiley-Interscience Publication, John Wiley & Sons, Inc.
- Breiman, L. 2001. “Random Forest.” *Machine Learning* 45: 5–32.
- Bruijnzeel, L., W. Eugster, and R. Burkard. 2006. *Fog as a Hydrologic Input*, 559–582. John Wiley & Sons.
- Chaloner, T. M., S. J. Gurr, and D. P. Bebbler. 2021. “Plant Pathogen Infection Risk Tracks Global Crop Yields Under Climate Change.” *Nature Climate Change* 11, no. 8: 710–715.
- Che, H., X. Zhang, Y. Li, and Z. Zhou. 2006. “Relationship Between Horizontal Extinction Coefficient and PM10 Concentration in Xi’an, China.” *China Particulogy* 4: 327–329.
- Chen, H., Y. Huang, H. Z. Shen, et al. 2017. “Modelling Temporal Variations in Global Residential Energy Consumption.” *Applied Energy* 184: 820–829.
- Cutler, A., D. Cutler, and J. Stevens. 2012. “Random Forests.” In *Ensemble Machine Learning*, edited by C. Zhang, and Y. Q. Ma, 157–175. Springer.
- Egli, S., B. Thies, and J. Bendix. 2018. “A Hybrid Approach for Fog Retrieval Based on a Combination of Satellite and Ground Truth Data.” *Remote Sensing* 10: 628.
- Egli, S., B. Thies, J. Drönner, J. Cermak, and J. Bendix. 2017. “A 10-Year Fog and Low Stratus Climatology for Europe Based on Meteosat Second Generation Data.” *Quarterly Journal of the Royal Meteorological Society* 143: 530–541.
- Fuchs, J., H. Andersen, J. Cermak, E. Pauli, and R. Roebeling. 2022. “High-Resolution Satellite-Based Cloud Detection for the Analysis

of Land Surface Effects on Boundary Layer Clouds.” *Atmospheric Measurement Techniques* 15: 4257–4270.

Gautam, R., and M. K. Singh. 2018. “Urban Heat Island Over Delhi Punches Holes in Widespread Fog in the Indo-Gangetic Plains.” *Geophysical Research Letters* 45: 1114–1121.

Gray, E., S. Gilardoni, D. Baldocchi, B. C. McDonald, M. C. Facchini, and A. H. Goldstein. 2019. “Impact of Air Pollution Controls on Radiation Fog Frequency in the Central Valley of California.” *Journal of Geophysical Research: Atmospheres* 124, no. 11: 5889–5905. <https://doi.org/10.1029/2018JD029419>.

Gultepe, I., R. Tardif, S. C. Michaelides, et al. 2007. “Fog Research. A Review of Past Achievements and Future Perspectives.” *Pure and Applied Geophysics* 164: 1121–1159.

Hess, M. F. 1965. *Vertical Climatic Zones in the Polish Western Carpathians*. Vol. 11, 195–198. Zesz Nauk UJ, [in Polish].

IMGW-PIB. n.d. Accessed January 8, 2024. https://danepubliczne.imgw.pl/data/dane_pomiarowo_obserwacyjne/dane_meteorologiczne/dobowe/synop/.

Klemm, O., and N. Lin. 2016. “What Causes Observed Fog Trends: Air Quality or Climate Change?” *Aerosol and Air Quality Research* 16: 1131–1142.

Lakra, K., and K. Avishek. 2022. “A Review on Factors Influencing Fog Formation, Classification, Forecasting, Detection and Impacts.” *Rendiconti Lincei. Scienze Fisiche e Naturali* 33, no. 2: 319–353.

Li, Z., J. Yang, and S. Huang. 2000. “Influence of Urban Aerosols With Humidity Effect on Temperature During Daytime.” *Chinese Journal of Atmospheric Sciences* [in Chinese] 24, no. 1: 87–94.

Lorenc, H., ed. 2012. *Natural Disasters and Internal Security (Civil and Economic) of the Country*, 7–32. IMGW-PIB [in Polish].

Lupikasza, E., and T. Niedzwiedz. 2016. “Synoptic Climatology of Fog in Selected Locations of Southern Poland (1966–2015).” *Bulletin of Geography Physical Geography Series* 10: 5–15.

Markowicz, K. M., I. Okrasa, M. T. Chilinski, P. Makuch, K. Nurowska, and O. Zawadzka-Manko. 2023. “Long-Term Variability of the MERRA-2 Radiation Budget Over Poland in Central Europe.” *Acta Geophysica* 72, no. 4: 2907.

Markowicz, K. M., O. Zawadzka, M. Posyniak, and J. Uscka-Kowalkowska. 2019. “Long-Term Variability of Aerosol Optical Depth in the Tatra Mountain Region of Central Europe.” *Journal of Geophysical Research: Atmospheres* 124: 3464–3475.

Markowicz, K. M., O. Zawadzka-Manko, and M. Posyniak. 2022. “A Large Reduction of Direct Aerosol Cooling Over Poland in the Last Decades.” *International Journal of Climatology* 42, no. 7: 4129–4146.

Me, F., A. Bokwa, A. Wypych, and M. J. Hajto. 2021. “Change of Fog Frequency.” In *Climate Change in Poland*. Springer Nature Switzerland AG.

Middleton, W. E. K. 1947. *Visibility in Meteorology: The Theory and Practice of the Measurement of the Visual Range*. University of Toronto Press.

National Centers for Environmental Information. n.d. Accessed January 8, 2024. <https://www.ncei.noaa.gov/pub/data/noaa/>.

NCEI’s Climate Data Online system. n.d. Accessed January 8, 2024. <https://www.ncei.noaa.gov/cdo-web/>.

Nurowska, K., and K. M. Markowicz. 2024. “Determination of Hygroscopic Aerosol Growth Based on the OPC-N3 Counter.” *Atmosphere* 15, no. 1: 61.

Osinski, S. 2004. “Changes in Poland’s Industry After 1989.” *Miscellanea Geographica* 11: 249–261.

Pauli, E., H. Andersen, J. Bendix, J. Cermak, and S. Egli. 2020. “Determinants of Fog and Low Stratus Occurrence in Continental Central Europe—A Quantitative Satellite-Based Evaluation.” *Journal of Hydrology* 591: 125451.

- Pedregosa, F., G. Varoquaux, A. Gramfort, et al. 2011. "Scikit-Learn: Machine Learning in Python." *Journal of Machine Learning Research* 12: 2825–2830.
- Peking University Repository. n.d. "Peking University Repository." Accessed September 13, 2023. <http://inventory.pku.edu.cn/download/download.html>.
- Pérez-Díaz, J. L., O. Ivanov, Z. Peshev, et al. 2017. "Fogs: Physical Basis, Characteristic Properties, and Impacts on the Environment and Human Health." *Water* 9, no. 10: 807. <https://www.mdpi.com/2073-4441/9/10/807>.
- Petrou, I., P. Kassomenos, and C. C. Lee. 2022. "Trends in Air Mass Frequencies Across Europe." *Ortical and Applied Climatology* 148: 105–120.
- PKU. n.d. "PKU Sources of Pollutants." Accessed September 13, 2023. <http://inventory.pku.edu.cn/Table%202.pdf>.
- Reizer, M., and K. Juda-Rezler. 2016. "Explaining the High PM10 Concentrations Observed in Polish Urban Areas." *Air Quality, Atmosphere and Health* 9: 517–531.
- Seinfeld, J. H., and S. N. Pandis. 2006. *Atmospheric Chemistry and Physics: From Air Pollution to Climate Change*. 2nd ed. John Wiley & Sons.
- Shi, C., M. Roth, H. Zhang, and Z. Li. 2008. "Impacts of Urbanization on Long-Term Fog Variation in Anhui Province, China." *Atmospheric Environment* 42, no. 36: 8484–8492.
- Shrestha, S., M. Peel, and G. Moore. 2022. "Cold Waves in Terai Region of Nepal and Farmer's Perception of the Effect of Fog Events and Cold Waves on Agriculture." *Ortical and Applied Climatology* 11, no. 151: 29–45.
- Skomorowski, A., and P. Piotrowski. 2018. "The Occurrence of Fog at Meteorological Stations Located on the Airport in Poland in the Years 2005–2015." *Przegląd Geofizyczny* 63: 315–327.
- Smith, A., N. Lott, and R. Vose. 2011. "The Integrated Surface Database: Recent Developments and Partnerships." *Bulletin of the American Meteorological Society* 92: 704–708.
- Trzeciak, S. 1992. "Fogs and Phenomena Accompanying Them in the Western Part of the Polish Baltic Coast." *Szczecinskie Roczniki Naukowe (Annales Scientiarum Stetinenses)* [in Polish] 7, no. 1: 67–85.
- Ustrnul, Z., D. Czekierda, and A. Wypych. 2010. "Extreme Fog Events in Poland With Respect to Circulation Conditions." In *EMS Annual Meeting Abstracts*, Vol. 7. 10th EMS / 8th ECAC.
- Ustrnul, Z., A. Wypych, and D. Czekierda. 2013. "Composite Circulation Index of Weather Extremes (the Example for Poland)." *Meteorologische Zeitschrift* 22: 551–559.
- Ustrnul, Z., A. Wypych, E. Henek, M. Maciejewski, and B. Bochenek. 2015. "Climatologically Based Warning System Against Meteorological Hazards and Weather Extremes: The Example for Poland." *Natural Hazards* 77: 1711–1729.
- Vautard, R., P. Yiou, and G. van Oldenborgh. 2009. "Decline of Fog, Mist and Haze in Europe Over the Past 30 Years." *Nature Geoscience* 2: 115–119.
- Wang, R., S. Tao, P. Ciais, et al. 2013. "High-Resolution Mapping of Combustion Processes and Implications for CO2 Emissions." *Atmospheric Chemistry and Physics* 13: 5189–5203.
- van der Werf, G. R., J. T. Randerson, L. Giglio, et al. 2010. "Global Fire Emissions and the Contribution of Deforestation, Savanna, Forest, Agricultural, and Peat Fires (1997–2009)." *Atmospheric Chemistry and Physics* 10: 11707–11735.
- Wielgosinski, G., and J. Czerwinska. 2020. "Smog Episodes in Poland." *Atmosphere* 11: 277.
- WMO. 2010. "Guidelines on Early Warning Systems and Application of Nowcasting and Warning Operations. WMO/TD 2010; No.1559."
- Wrzesinsky, T., and O. Klemm. 2000. "Summertime Fog Chemistry at a Mountainous Site in Central Europe." *Atmospheric Environment* 34: 1487–1496.
- Wypych, A. 2003. "Air Humidity and Fogs in Cracow in the Period 1961–2000 in Relation to Synoptic Situations." In *Changes of Geographical Environment and Those of Socio-Economic Phenomena*, edited by Z. Gorka, vol. 112, 105–114. Zesz Nauk UJ.
- Yan, S., B. Zhu, Y. Huang, et al. 2020. "To What Extents Do Urbanization and Air Pollution Affect Fog?" *Atmospheric Chemistry and Physics* 20: 5559–5572.
- Yan, S., B. Zhu, and H. Kang. 2019. "Long-Term Fog Variation and Its Impact Factors Over Polluted Regions of East China." *Journal of Geophysical Research: Atmospheres* 124: 1741–1754.
- Zarnowiecki, G. 2000. "The Occurrence of Days With Fog in Swiety Krzycz, Kielce and Nowa Slupia." *Rocznik Świątokrzyski. Seria B* [in Polish] 27: 265–279.

Appendix A

Theoretical Model

Fog phenomena can be theoretically reported during intensive aerosol episodes below saturated conditions (RH < 100%). To estimate the PM₁₀ mass concentration, which can be responsible for the reduction of visibility below 1 km we used the Koschmieder equation (Middleton 1947; Che et al. 2006). It describes an algebraic relationship between visibility (VIS) and the light extinction coefficient (σ)

$$\sigma = \frac{\ln(50)}{VIS}. \quad (A1)$$

According to the Lorentz-Mie theory (Bohren and Huffman 1983) the relationship between particle extinction coefficient and PM₁₀ mass concentration can be done for spherical particles. The extinction coefficient can be calculated from

$$\sigma = \pi \int Qr^2 N(r) dr, \quad (A2)$$

where $N(r)$ is particle size distribution, and Q is particle effective cross-section. The PM₁₀ is defined as

$$PM_{10}(RH) = \frac{4}{3} \pi \int \rho r^3 N(r) dr, \quad (A3)$$

where ρ is particle density. By definition of effective particle radius, the relationship between PM₁₀ and σ can be written in the following simplification form

$$PM_{10}(RH) = \frac{4\rho r_{eff} \ln(50)}{3 < Q > VIS}, \quad (A4)$$

where $< Q >$ is the mean particle effective cross-section for a given particle size distribution and light refractive index. The PM₁₀ (RH) corresponds to the ambient condition while in air quality monitoring this quantity is defined for dry (RH < 50%) conditions. Therefore, it must be converted to dry condition with the use of the particle growth factor:

$$PM_{10} = \frac{PM_{10}(RH)}{GF}, \quad (A5)$$

$$GF(RH) = 1 + \kappa \frac{\rho_w / \rho}{100/RH - 1},$$

where σ_w is water density, κ is a hygroscopic parameter. To estimate the PM₁₀ mass concentration at 1 km visibility we assumed aerosol size distribution measured by LAS4031 sensor in Warsaw and a refractive index of 1.52 + 0.005i. The Kappa hygroscopic parameter is assumed of 0.12 ± 0.17 based on observation in Warsaw reported by (Nurowska and Markowicz 2024).

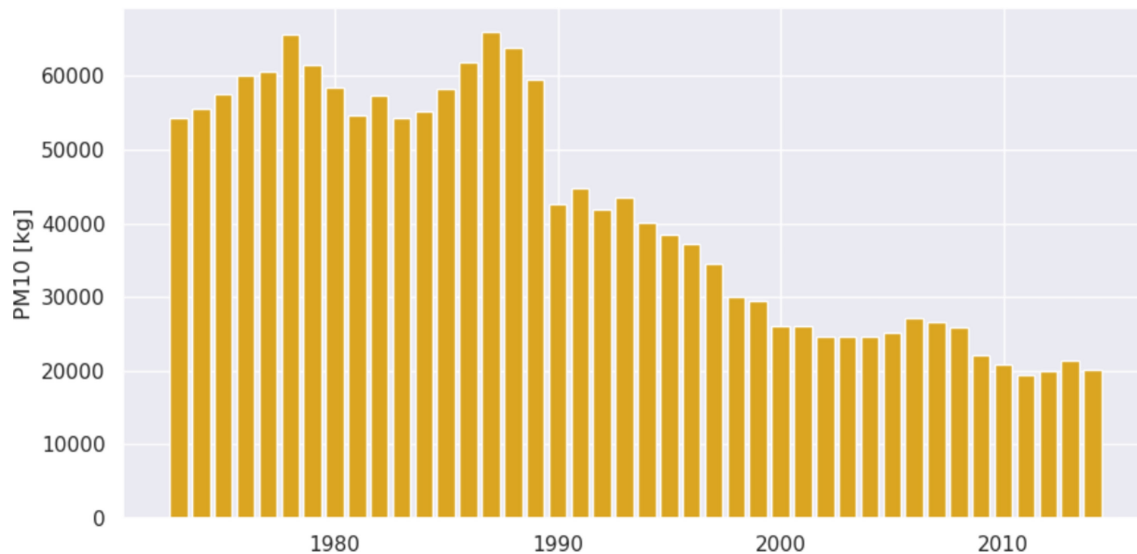


FIGURE A1 | PM_{10} annual emissions for years 1973–2020, calculated as a mean from all stations, based on PKU Inventory data. [Colour figure can be viewed at [wileyonlinelibrary.com](https://onlinelibrary.wiley.com)]

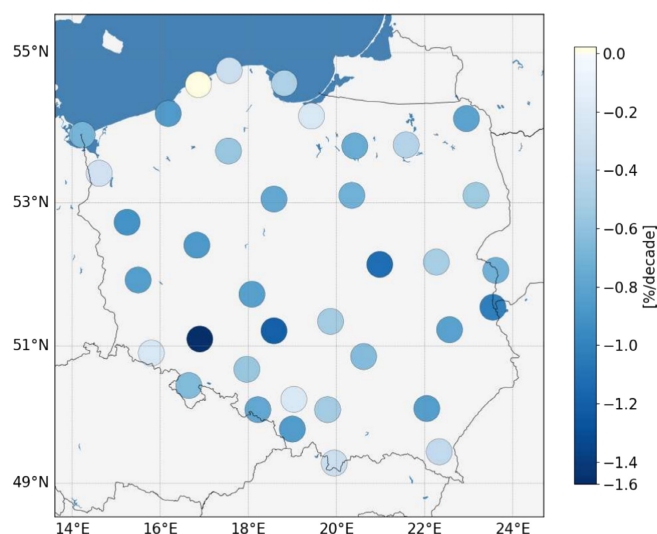


FIGURE A2 | Trend of the RH [%/decade] for years 1973–2020. [Colour figure can be viewed at [wileyonlinelibrary.com](https://onlinelibrary.wiley.com)]

TABLE A1 | Mean trends for different station types for days with wind speed < 3 m/s, days with RH = 100%, days with favourable conditions (windspeed < 3 m/s and RH = 100%), RH [%] before and after 1990.

Station type	Days with windspeed < 3 [m/s]		Days with RH = 100 [%]		Days with fav. cond. ws < 3 [m/s] and RH = 100 [%]		RH [%]	
	Before	After	Before	After	Before	After	Before	After
Background	5.51 (1.42)	0.46 (0.32)	-8.1 (4.76)	2.55 (2.58)	-7.07 (4.23)	1.87 (3.08)	-0.36 (0.96)	-0.63 (0.32)
Mountains	2.73 (1.91)	0.2 (0.16)	-2.05 (0.92)	-0.69 (0.39)	-2.94 (2.25)	-0.16 (1.73)	-0.9 (1.0)	-0.41 (0.54)
Seaside	0.91 (1.7)	0.14 (0.28)	-13.08 (3.03)	2.18 (2.99)	-13.25 (3.44)	2.04 (2.94)	-0.38 (0.47)	-0.83 (0.6)
Suburban	1.16 (2.4)	0.4 (0.4)	-7.69 (4.12)	1.36 (2.92)	-7.32 (4.17)	1.51 (2.68)	-0.27 (0.93)	-1.03 (0.54)
Urban	1.71 (2.4)	0.34 (0.21)	-10.04 (4.34)	3.37 (2.76)	-9.63 (4.14)	3.58 (2.79)	-0.42 (0.77)	-0.73 (0.44)
POLAND	1.88 (2.56)	0.35 (0.33)	-8.63 (4.55)	1.92 (2.85)	-8.3 (4.52)	1.96 (2.78)	-0.36 (0.83)	-0.86 (0.51)
Mountains excl.	1.83 (2.61)	0.36 (0.34)	-8.98 (4.39)	2.06 (2.85)	-8.59 (4.45)	2.08 (2.79)	-0.33 (0.82)	-0.88 (0.51)

Note: In brackets, standard deviations are given.